Transient Simulation of Multi-Physical Field Coupling in Electrochemical Machining Microstructure

Xiang LI*, Xinyu WEN**, Yuanlong CHEN**, Hua LIN***
*School of Intelligent Manufacturing, Anhui Vocational and Technical College, No. 2600, Wenzhong Road, Hefei 230011, Anhui Province, China, E-mail: lix1117@163.com (Corresponding Author)
**School of Mechanical Engineering, Hefei University of Technology, No. 193, Tunxi Road, Hefei 230009, Anhui Province, China
***School of Mechanical and Automotive Engineering, West Anhui University, No. 237000, Yunlu Bridge West Moonlight Island, Lu'an 237000, Anhui Province, China, E-mail: linhua5704@hotmail.com

1. Introduction

Microstructures are commonly found on precision parts in aerospace, chemical equipment, precision machinery and biomedical fields. Its machining accuracy has an important impact on the performance of the parts [1]. Typically, microstructures are prepared by laser machining, micro-milling and electrochemical machining. Compared with technologies such as micro-milling and laser machining, electrochemical machining is an ideal method for machining microstructures by virtue of its advantages such as wide machining range, high efficiency, good machined surface quality, no loss of tool cathode and no macroscopic cutting force [2]. Therefore, many scholars have carried out a lot of research on electrochemical machining

He et al. [3] utilized the mask-jet electrochemical machining technique to process microporous arrays on Zr702 thin plates. The dissolution characteristics of Zr702 in different concentrations of NaNO₃ and NaCl electrolytes were investigated. The evolution of the microporous cross-sectional profile is analyzed by 2D modeling, which yields a high quality microporous array with a depth-to-diameter ratio of 0.501. Mayank et al [4] investigated the law of bubble effects on electrolyte conductivity and material removal rate in electrochemical processing.

Jiang et al. [5] performed low-frequency vibration of cathode tools to enhance bubble removal and electrolyte renewal in electrochemical machining, which improved blade machining contour accuracy and surface quality. Manikandan et al [6] used grey correlation analysis to optimize the mathematical model of electrolytic machining feed rate, electrolyte flow rate, and electrolyte concentration on the material removal rate and machining gap and obtained a better combination of parameters.

Yahyavi Zanjani et al [7] found that the current density can be controlled by adjusting the electrolytic machining process parameters to machine the grooves with desired depth and surface roughness. Patel [8] performed simulations to go to get the current density distribution pattern during electrochemical machining of micro-pits. Finally, micro-pits with width of 115-160 μm were machined in stainless steel substrate.

Rahman et al [9] used cylindrical tungsten electrodes in electrochemical machining to analyze the effect of process parameters on the overcut and diameter of microholes. Taguchi technique was used to optimize the machining parameters and to develop a regression model. High quality holes were machined under the optimized parameters, which had a diameter of 413 μm and an overcut of 70 μm

Wang et al. [10] proposed a novel variable-parameters blisk ECM strategy based on the synchronous coupling mode of micro-vibration amplitude and small pulse duration to investigate the effect of machining gap on electrochemical machining blisk, resulting in blades with high profile accuracy and surface quality. Rathod et al [11] used a columnar tungsten electrode with a diameter of 140 μm for electrochemical machining of microgrooves. Grooves with a width of 150 μm and a line roughness of 0.104 μm on the bottom surface of the groove were machined at a machining voltage of 2.6 V, a pulse frequency of 8 MHz, a duty cycle of 30%, and a scanning speed of 93.75 mm·s⁻¹.

As shown above, it is easy to study the specific working conditions by experimental methods. However, the electric field between the electrodes, the distribution of the flow field and the electrochemical reaction process will lead to the machining gap distribution is extremely uneven and the rule of law is complex in electrochemical machining. Therefore, it is very difficult to monitor and control the electrochemical machining process. This paper investigates the multi-physics field coupling law of microstructural electrochemical machining to improve guidance for future experimental analysis.

2. Mathematical Modeling of Multi-Physics Fields for Electrochemical Machining of Microstructures

Electrochemical machining is a specialty machining method that utilizes the principle of anodic dissolution of metals in an electrolytic solution to machine workpieces. In electrochemical machining, the electric field in the electrolyte is regarded as a passive electric field, the conductivity of the electrolyte remains constant and isotropic, and the current efficiency of the electrolyte is approximately constant. From the basic theory of electric field, it is known that the distribution of electric field potential ϕ in the whole machining area is in accordance with Laplace [12]:

$$\frac{\partial^2 \phi}{\partial x^2} + \frac{\partial^2 \phi}{\partial y^2} + \frac{\partial^2 \phi}{\partial z^2} = 0 . \tag{1}$$

In the study of gas-liquid two-phase flow in the electrochemical machining gap, only hydrogen bubbles pre-

cipitated at the cathode are considered. Meanwhile, an easily convergent turbulent bubble flow model is used to study the distribution law of the gas-liquid two-phase flow field during electrochemical machining. The mass flux of hydrogen produced on the surface of the cathode tool per unit time and area can be calculated by the following equation [13]:

$$N_{H2} = \frac{M \eta i}{2F},$$ (2)

where N_{H2} is the hydrogen flux, M is the hydrogen molar mass, i is the current density, F is the Faraday constant and η is the current efficiency.

The heat generated in electrochemical machining comes from two main sources: the Joule heat generated by the current in the machining gap and the heat generated by the electrode reaction. As the heat generated by the latter is small and negligible, it satisfies the convection-diffusion equation:

$$\rho c_p \frac{\partial T}{\partial t} + \rho c_p v \nabla T = \nabla (k \nabla T) + Q_{Joule} + Q_{Reaction},$$ (3)

where c_p is the specific heat capacity of the electrolyte, Q_{Joule} is the Joule heat generated during machining, $Q_{Reaction}$ is the heat of reaction.

The conductivity of the electrolyte is affected by the amount of hydrogen and the temperature rise of the electrolyte, resulting in an uneven distribution of conductivity, which in turn affects the current density distribution. The relationship between the conductivity, temperature and hydrogen content of the electrolyte is summarized in the following equation [14]:

$$\kappa = \kappa_0 \left[1 + \alpha (T_1 - T_0) \right] (1 - \beta)^n,$$ (4)

where κ is the electrolyte conductivity, κ_0 is the initial conductivity of the electrolyte, α is the temperature coefficient of conductivity, the value is generally 0.02~2.00, T is the temperature of the electrolyte, T_0 is the initial temperature of the electrolyte, β is the bubble rate, n is the index of the effect of the bubble rate on the conductivity, $n = 1.5$~2.0.

3. Multi-Physics Field Modeling

Electrochemical machining involves multi-physical field coupling, it is difficult to observe the distribution law and change trend of each physical field in real time. Through the establishment of multi-physical field model and simulation to analyze the mutual influence relationship between the physical fields, indirectly reflecting the change rule of machining parameters to predict the electrochemical machining.

Electrochemical machining involves gas-liquid-solid three-phase flow. Due to the small volume ratio occupied by the anode product in microstructure machining, its effect can be neglected. Therefore, it can be simplified to a gas-liquid two-phase flow problem when simulated using simulation software, and the model can be simplified to two dimensions, as shown in Fig. 1. In the electrochemical machining simulation, it is assumed that the machining has entered the machining equilibrium state to facilitate the modeling and analysis of the physical field distribution law.
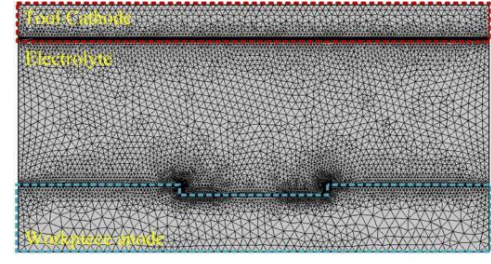

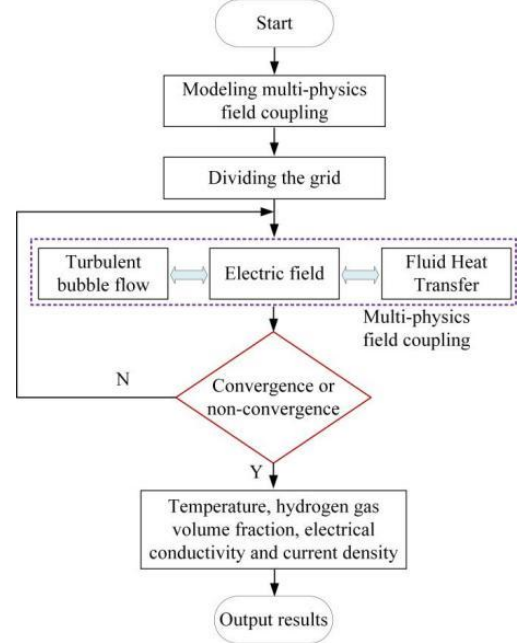Fig. 1 Geometric model of electrochemical machining simulation

Fig. 2 Multi-physics field coupled model solving process

The liquid-phase velocity field calculated using bubble flow simulation was used as the initial condition for velocity in fluid heat transfer. The liquid-phase velocity field is combined with the current density of the electrolyte, thus realizing the three-phase coupling of electric field-flow field-temperature field. The simulation flow of electric field, gas-liquid two-phase flow field and temperature field is shown in Fig. 2. Simulation models of electric field, gas-liquid two-phase flow field and temperature field were established and meshed according to the machining requirements. Current, bubble flow, k~ε and fluid heat transfer module were selected in the software. Multi-physics field simulations were carried out using transients as studies.

4. Multi-Physics Field Coupling Simulation Research

In electrochemical machining, the anode workpiece and cathode tool materials are 304 stainless steel materials, electrolyte selection of sodium nitrate solution. In the simulation parameter selection, the machining voltage is 11 V, pulse duty cycle is 30%, power frequency is 5 kHz, machining gap is 0.5 mm, electrolyte inlet velocity is 0.8 m·s⁻¹ and the electrolyte concentration is 2.0 mol·L-1. When setting up the pulsed current in the coupled model, the solution step (1×10-5 s) is set to be smaller than the pulse period (2×10-4 s) to obtain a more accurate multi-physics field distribution. In this paper, the temperature field, gas-liquid two-phase flow field and electric field distributions are simulated for 10 cycles (0.002 s).

4.1. Temperature in the machining gap at different moments

The cloud diagram of the temperature distribution of the multi-physics field coupled simulation of electrochemical machining is shown in Fig. 3. As can be seen in Fig. 3, the temperature distribution is uneven within the machining gap, the temperature near the electrolyte inlet is almost unchanged, and it gradually increases along the flow direction, the temperature is maximum at the outlet, with a maximum temperature of 294.6 K. The temperature of the electrolyte at the exit is also higher than the temperature at the inlet. This is mainly due to the fact that the Joule heat and reaction heat generated in electrochemical machining are accumulated in the electrolyte, the flowing electrolyte carries the Joule heat and reaction heat generated in the process from the inlet to the outlet along the flow direction and accumulates at the outlet, where the temperature is greater than that at the inlet. At the top corner due to the aggregation effect of the current, the current density value is larger and relatively more Joule heat and reaction heat are generated. In addition, under fluid action, more heat accumulates near here and the temperature rise at the top corner is larger.

Fig. 4 shows the trend of temperature change along the process direction at different moments. As can be seen from Fig. 4, at the initial stage of machining, no electrochemical reaction occurs and there is almost no temperature rise in the machining gap. As the machining time increases, the current density between the poles gradually increases, the degree of electrochemical reaction increases, and therefore the Joule heat increases. The products eroded from the
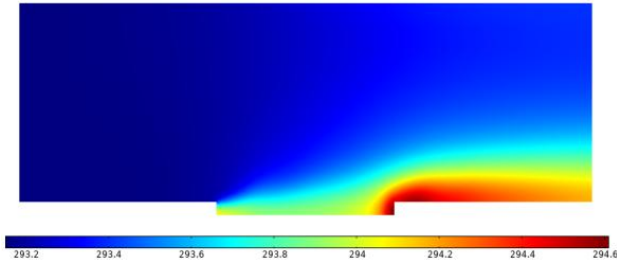

Fig. 3 Cloud of temperature distribution in electrochemical machining
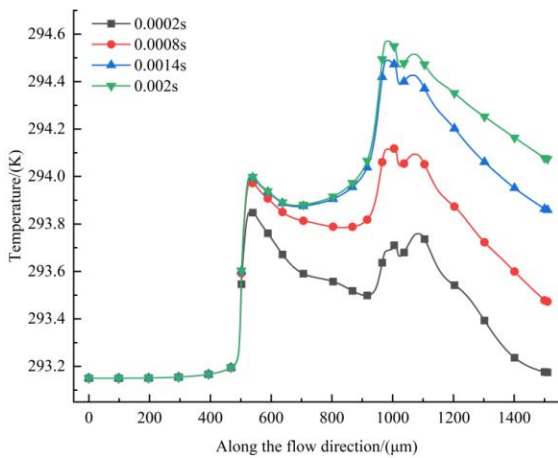

Fig. 4 Temperature variation at different moments along the flow direction

anode surface and the hydrogen precipitated from the cathode during machining are carried by the flowing electrolyte

from the inlet to the outlet along the process direction and accumulate at the outlet, resulting in higher temperatures near the outlet, so that the temperature gradually increases along the process direction.

4.2. Hydrogen content in the machining gap at different moments

In electrochemical machining when a large amount of electrolyte flows through the machining gap, the anode removes material and hydrogen gas precipitates on the cathode. The hydrogen gas produced disappears as part of the gas with the flow of electrolyte, and the other part of the gas reaches the exit position. The gas bubbles in the machining gap accumulate rapidly after energization, and the volume fraction of hydrogen gas shows a sequential increasing trend along the inlet to the outlet of the electrolyte, as shown in Fig. 5. The volume fraction of hydrogen gas at the inlet is the smallest, and its maximum occurs at the outlet of the electrolyte. The proportion of hydrogen volume fraction directly reflects the change of bubble rate, and the change of bubble rate affects the change of conductivity, which in turn affects the inter-pole current density.
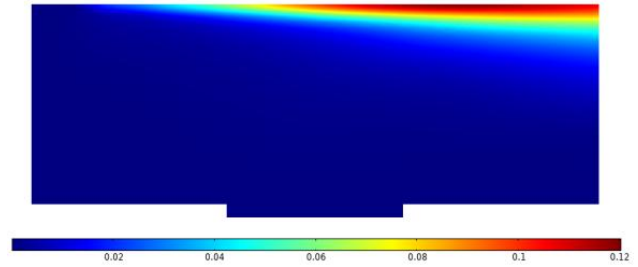

Fig. 5 Cloud of hydrogen volume distribution in electrochemical machining

Fig. 6 shows the trend of hydrogen volume fraction in the machining gap at different moments. It can be seen that at the initial stage of machining, only a slight degree of electrochemical reaction occurs at the anode electrolyte interface, and the amount of hydrogen at the cathode is negligible. At the inlet there is almost no hydrogen, with increasing hydrogen content along the process direction as the machining time increases, reaching a maximum of about 17% at the outlet. This is mainly due to the fact that in electrochemical machining, as the machining time increases, the current density gradually increases, the degree of electrochemical reaction occurring in the anode surface material gradually increases, the anode surface material is removed and hydrogen is gradually generated. On the one hand, as part of the hydrogen generated disappears with the flow of the electrolyte, the other part of the hydrogen is carried by the flowing electrolyte to the outlet position and accumulates. On the other hand, as the electrolyte is renewed in a more timely manner at the inlet location, the electrolysis products and hydrogen are carried away by the flowing electrolyte and eventually accumulate at the outlet location, which results in a gradual increase of hydrogen content in the process direction.

When the time is 0.0002 s, the bubbles flow through 160 μm under the flow of electrolyte, and with the increase of machining time, the bubbles initially accumulate in the runner and there is a sudden increase in the bubble rate at 200 μm. When the time is 0.0008 s, the higher current
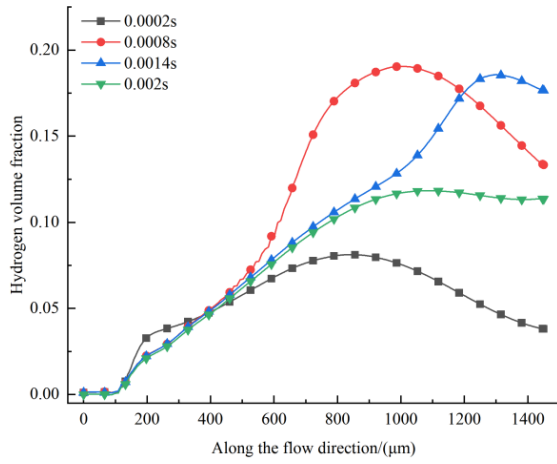
Fig. 6 Hydrogen content variation at different moments along the flow direction

Fig. 7 Cloud of electrolyte conductivity distribution in electrochemical machining

density in the middle produces more bubbles and the bubbles flow through 640 μm at the entrance of the runner. In addition, the bubbles precipitated from the cathodic reaction at this time make the bubble content larger at 600 μm-1000 μm, and the bubble rate peaks at 1000 μm. At time 0.0014 s, the electrolyte flow brings bubbles to the middle and back section and initially the channel inlet bubbles have been brought to the end of the channel at 1300 μm. Finally, at time 0.002 s, the initial flow channel inlet bubbles are completely discharged. At this time, the bubble generation and discharge to the equilibrium state, electrochemical machining into machining equilibrium.

4.3 Electrolyte conductivity in the machining gap at different moments

Combined with Eq (4) and Eq (6), it can be seen that the electrolyte conductivity is jointly affected by temperature and hydrogen content. The electrolyte conductivity is inversely proportional to the hydrogen volume fraction and directly proportional to the electrolyte temperature. That is to say, the electrolyte conductivity decreases with increasing hydrogen volume fraction and increases with increasing temperature. Fig. 7 is a cloud diagram of the electrolyte conductivity distribution for the multi-physics field coupling simulation of electrochemical machining. It can be seen from Fig. 7 that the electrolyte conductivity shows a decreasing trend along the electrolyte flow direction, with the maximum electrolyte conductivity at the inlet, gradually decreasing along the flow direction and the minimum at the outlet of the electrolyte, which shows an inverse trend with the hydrogen volume fraction. This is mainly due to the gradual increase in temperature generated in the electrochemical process and the gradual accumulation of hydrogen along the flow direction with the electrolyte flow. At the inlet, the conductivity is relatively high at the inlet due to the timely renewal of the electrolyte and the processed products being carried away. Process products are carried away to accumulate near the exit and the electrolyte conductivity is relatively low.

Fig. 8 shows the trend of electrolyte conductivity in the machining gap at different moments. It can be seen from Fig. 8 that the electrolyte conductivity shows a decreasing trend along the electrolyte flow direction and the electrolyte conductivity is always lower than the initial conductivity during the whole machining stage. At the initial
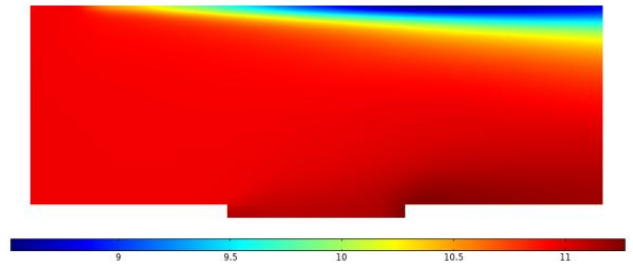
stage of machining, the electrochemical reaction at the anode electrolyte interface is slow, producing less hydrogen and the conductivity of the electrolyte is relatively uniformly distributed throughout the machining gap. As the machining time increases, the conductivity of the exit electrolyte gradually decreases. This is mainly due to the fact that as the machining time increases, the current density between the cathode and anode increases, and the degree of electrochemical reaction in the entire gap is more intense. The rate of removal of material from the anode surface and the generation of hydrogen gas from the cathode surface are higher, and a large amount of anode material is etched away while hydrogen ions in the solution get electrons on the cathode surface and undergo a reduction reaction to generate hydrogen gas. The precipitated hydrogen and Joule heat flow with the flowing electrolyte and eventually accumulate at the process outlet, which reduces the conductivity.

It can also be seen from Fig. 8 that the conductivity of the electrolyte is maximum at the entrance and decreases gradually along the process direction with the increase of the machining time and is minimum at the process exit. At the inlet, the conductivity is relatively high because the electrolyte is renewed in time and the hydrogen content and temperature are low. Along the flow direction, the hydrogen content and temperature gradually increase, combined with Fig. 4 and Fig. 5, it can be seen that the temperature change in the flow channel of the machining area is small and has little effect on the electrolyte conductivity, which has not increased the electrolyte conductivity. The hydrogen volume fraction in the flow channel in the machining area has a larger change and the electrolyte conductivity is more affected by the hydrogen volume fraction, so the electrolyte conductivity gradually decreases.

The change of electrolyte conductivity has the opposite trend to the change of bubble content. When the time is 0.0002 s, the bubbles flow through 160 μm under the flow of electrolyte, and with the increase of machining time, the bubbles initially accumulate in the runner, and the bubble rate increases abruptly at 200 μm, at which time the conductivity decreases rapidly. When the time is 0.0008 s, the higher current density in the middle produces more bubbles, and the bubbles flow through 640 μm at the entrance of the flow channel, coupled with the bubbles precipitated by the cathodic reaction at this time, making the bubble content of 600 μm-1000 μm larger, and the bubble rate peaks at 1000 μm, which corresponds to the lowest conductivity of the electrolyte. When the time is 0.0014 s, the electrolyte flow will bring the bubbles to the middle and back section, the conductivity gradually decreases and initially the bubbles at the entrance of the flow channel have been brought to the end of the flow channel at 1300 μm. Finally, at the time of 0.002 s, the initial flow channel inlet bubbles have
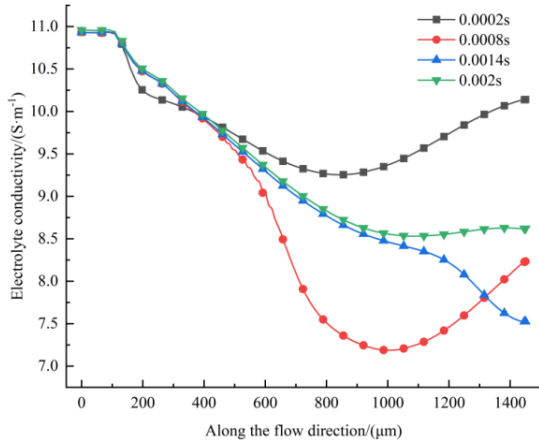
Fig. 8 Electrolyte conductivity at different moments along the flow direction

completely flowed out and the bubble generation and discharge reached a balanced state. However, the bubble content at this time was reduced compared with that at 0.0014 s and the conductivity was relatively increased.

4.4. Current density in the machining gap at different moments

In electrochemical machining, temperature and hydrogen content affect the electrolyte conductivity and hence the current density. Fig. 9 and Fig. 10 show the current density distribution cloud and the current density variation curves at different moments along the process direction. It can be seen from Fig. 9 and Fig. 10 that the current density in the unprocessed region is small and the current density in the processed region is large. As the machining time increases, the current density in the processed region gradually increases. This is mainly due to the fact that the resistance of the unprocessed region is higher compared to the processed region, so the current density in this region is smaller.

In the machining area, with the increase of machining time, the current density gradually shows the trend of increasing and then decreasing. This is mainly due to electrochemical machining starting order machining area, the anode electrolyte interface only a slight degree of electrochemical reaction occurs, so at this time in the interface at the current density is small. As the machining time increases, the electrochemical reaction time increases and the current density increases. However, as the reaction time continues to increase, the degree of electrochemical reaction intensifies, the surface of the metal anode material is constantly oxidized, and the anode material is eroded. And the tool cathode interface precipitated hydrogen gas with the electrolyte flow at the outlet accumulation, electrolyte conductivity and current density decreased.

5. Conclusions

Electrochemical machining is a machining method that utilizes the continuous dissolution of the metal at the anode and the final shaping of the metal. The machining has different effects on the electric field, flow field and temperature field due to the precipitation of hydrogen from the cathode. In electrochemical machining, the electric field, flow field and electrochemical factors not only interact with each other, but also change continuously with time and
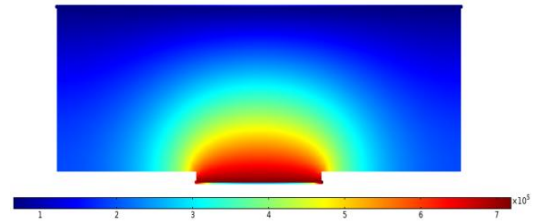

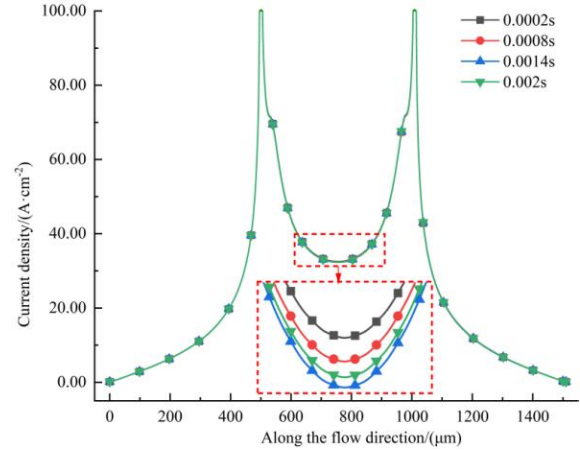Fig. 9 Cloud of current density distribution in electrochemical machining

Fig. 10 Current density variation at different moments along the flow direction

space, making it difficult to sample and test them in real time during the machining process. Therefore, the electrochemical theoretical analysis and simulation carried out in the paper are based on certain simplifications the assumptions and the guiding law given can only be qualitative with certain reference value.

Along the flow direction, the temperature and hydrogen content in the processing gap gradually increase, and the electrolyte conductivity and current density gradually decrease. This is mainly due to the fact that the Joule heat generated by the electric current and electrode reactions are carried by the flowing electrolyte from the inlet to the outlet and accumulated at the outlet, which leads to a gradual increase in temperature along the flow direction. In electrochemical machining, the cathode continuously precipitates hydrogen, which is carried by the flowing electrolyte from the inlet to the outlet and accumulates at the outlet, which results in a gradual increase in hydrogen content in the flow direction. Electrolyte conductivity is affected by both temperature and hydrogen content. However, the trend of temperature rise is smaller than the trend of increasing hydrogen content, so the temperature has less effect on the electrolyte conductivity than hydrogen has on it, that is to say, the more hydrogen content there is, the less electrolyte conductivity there is. So along the flow direction, the electrolyte conductivity gradually decreases. Current density is positively correlated with electrolyte conductivity. Therefore, along the flow direction, the current density gradually decreases.

Acknowledgements

Conflict of Interest

The authors declare that they have no known competing financial interests or personal relationships that could have appeared to influence the work reported in this paper.

References

1. **Ge, Z.; Chen, W.; Zhu, Y.** 2022. Simulation and Experimental Study on Improving Electrochemical Machining Stability of Highly Convex Structures on Casing Surfaces Using Backwater Pressure, Chinese Journal of Mechanical Engineering 35: 98.
   https://doi.org/10.1186/s10033-022-00752-x.
2. **Chen, Y. L.; Li, X.; Zhang, Y. C.; Liu, J. Y.** 2022. Effects of Machining Parameters on Electrochemical Multi-Field Coupling, Mechanika 28(6): 473-480.
   https://doi.org/10.5755/j02.mech.31499.
3. **He, J.; Wang, Z.; Wang, J.; Liang, H.; Lian, H.** 2023. Investigation of the microhole arrays generated by masked jet electrochemical machining with polyaluminum chloride electrolyte, Precision Engineering 82: 370-382.
   https://doi.org/10.1016/j.precisioneng.2023.05.001.
4. **Mayank G.; Kunieda M.** 2017. Two-Phase Simulation of Electrochemical Machining, International Journal of Electrical Machining 22: 31-35.
   https://doi.org/10.2526/ijem.22.31.
5. **Jiang, X.; Li, Y.; Li, D.; Xu, Z.** 2023. Influence of machining gap on both sides of blade in vibration-assisted pulsed electrochemical machining, International Journal of Electrochemical Science 18(5): 100125.
   https://doi.org/10.1016/j.ijoes.2023.100125.
6. **Manikandan, N.; Kumanan, S.; Sathiyanarayanan, C.** 2017. Multiple performance optimization of electrochemical drilling of Inconel 625 using Taguchi based Grey Relational Analysis, Engineering Science and Technology, an International Journal 20(2): 662-671.
   https://doi.org/10.1016/j.jestch.2016.12.002.
7. **Zanjani, M. Y.; Hackert-Oschätzchen, M.; Martin, A.; Meichsner, G.; Edelmann, J.; Schubert, A.** 2019. Process Control in Jet Electrochemical Machining of Stainless Steel through Inline Metrology of Current Density, Micromachines 10(4): 261.
   https://doi.org/10.3390/mi10040261.
8. **Patel, D. S.; Agrawal, V.; Ramkumar, J.; Jain, V. K.; Singh, G.** 2020. Micro-texturing on free-form surfaces using flexible-electrode through-mask electrochemical micromachining, Journal of Materials Processing Technology 282: 116644.
   https://doi.org/10.1016/j.jmatprotec.2020.116644.
9. **Rahman, M. Z.; Das, A. K.; Chattopadhyaya, S.** 2021. Machinability study of stainless steel in deep micro-holes fabrication through μECM using balance electrode, Materials Today: Proceedings 43: 1437-1442.
   https://doi.org/10.   1016/j.matpr.2020.09.181.
10. **Wang, J.T.; Xu, Z.Y.; Zhu D.** 2023. Improving profile accuracy and surface quality of blisk by electrochemical machining with a micro inter-electrode gap, Chinese Journal of Aeronautics 36(4): 523-537.
    https://doi.org/10.1016/j.cja.2022.07.005.
11. **Rathod, V.; Doloi, B.; Bhattacharyya, B.** 2015. Experimental investigations into machining accuracy and surface roughness of microgrooves fabricated by electrochemical micromachining, Proceedings of the Institution of Mechanical Engineers, Part B: Journal of Engineering Manufacture, 229(10): 1781-1802.
    https://doi.org/10.1177/0954405414539486.
12. **Zhou, S.; Wang, D.; Cao, W.; Zhu, D.** 2023. Investigation of anode shaping process during co-rotating electrochemical machining of convex structure on inner surface, Chinese Journal of Aeronautics 36(7): 489-504.
    https://doi.org/10.1016/j.cja.2022.08.008.
13. **Liu, G.D.; Tong, H.; Li, Y.; Zhong, H.; Tan, Q.** 2020. Multiphysics research on electrochemical machining of micro holes with internal features, The International Journal of Advanced Manufacturing Technology 110: 1527-1542.
    https://doi.org/10.1007/s00170-020-05973-9.
14. **Zong, Y.Y.; Liu J.; Zhu, D.** 2021. Study of voltage regulation strategy in electrochemical machining of blisk channels using tube electrodes, The International Journal of Advanced Manufacturing Technology 114: 3489-3501.
    https://doi.org/10.1007/s00170-021-07065-8.

X. Li, X.Y. Wen, Y.L. Cheng, H. Lin

TRANSIENT SIMULATION OF MULTI-PHYSICAL FIELD COUPLING IN ELECTROCHEMICAL MACHINING MICROSTRUCTURE

S u m m a r y

Microstructural electrochemical machining involves electric field, temperature field and gas-liquid two-phase flow field with complex coupling relationship. At present, there is no mature technology that can control processes such as ion exchange and liquid-phase mass transfer in the machining. Therefore, in order to better understand the role of multi-field coupling and machining mechanism in microstructural electrochemical machining, a simulation study based on the multi-physics field coupling model is carried out to reveal the multi-physics field distribution law, which provides a guide for the subsequent research.

Keywords: electrochemical machining, multiphysical field coupling, temperature, hydrogen volume fraction, electrolyte conductivity, current density.